Multiple model control of a Buck dc/dc converter

D. Alejo, P. Maussion*,[1], J. Faucher[1]

Laboratoire d'Electrotechnique et d'Electronique Industrielle de Toulouse, Unité Mixte de Recherche INPT-ENSEEIHT (Ecole Nationale Supérieure d'Electrotechnique, Electronique, Informatique Hydraulique et Télécoms)/CNRS No. 5828, BP 7122-2, rue Camichel, 31071 Toulouse Cedex 7, France

Abstract

This paper describes a new method for algorithms commutation between two linear laws, for the voltage control of a dc/dc converter with variable loads. A multiple model control (MMC) is the generated, based upon the fusion of only two traditional IP controllers outputs. This strategy improves the performances of the step input responses and robustness.

Keywords: IP controllers; Fuzzy logic; Fusion; Multiple model control

1. Introduction

The object of this article is not so much the development of a new method for a dc/dc converter control, but rather than the test of feasibility of an original multiple model control principle: how to improve the performances by a progressive mixture of two very simple controllers? The use of fuzzy logic generally gives the opportunity to combine various laws for the same system [1–4]. Based upon the fuzzy logic principles (membership function), this work presents for this type of static inverter of power, a very simple fusion of two traditional control laws with supervision in order to improve the dynamic performances. A special procedure is defined to compute the model membership function degree.

* Corresponding author.
E-mail addresses: dominique.alejo@leei.enseeiht fr, pascal maussion@leei.enseeiht fr (P. Maussion), jean.faucher@leei.enseeiht fr (J. Faucher).
URL: http://www.leei.enseeiht fr.
[1] Tel.: +33-561-58-8354; fax: +33-561-63-8895.

Nomenclature	
C	output capacitor 165 μF
C_1	IP controller for $R = 10\,\Omega$
C_2	IP controller for $R = 200\,\Omega$
C_e	input capacitor 1000 μF
d_1	distance between model 1 and the system
d_2	distance between model 2 and the system
E	supply voltage
Fa_1	membership function degree for model no. 1
Fa_2	membership function degree for model no. 2
I_s	output current
Il	inductor current
Il_ref	inductor current reference
Il_mes	inductor current measure
L	output inductor 2.23 mH
M_1	model with $R = 10\,\Omega$
M_2	model with $R = 200\,\Omega$
P_1	input filter no. 1 for reference
P_2	input filter no. 2 for reference
R_1, & R_2	output resistors 200 and 10 Ω
T & D	IGBT
T_c	MosFet for load connection or disconnection
u	MMC signal control
u_1	IP signal control for $R = 10\,\Omega$
u_2	IP signal control for $R = 200\,\Omega$
V_mes	output voltage measure
V_ref	output voltage reference
V_s	output voltage
V_{s_1}	output voltage for model 1 with $R = 10\,\Omega$
V_{s_2}	output voltage for model 2 with $R = 200\,\Omega$
Greek letter	
Σ	real system

2. System description

The system under control is a 1 kW non-reversible Buck dc/dc converter presented on Fig. 1. As the converter is used in current mode control, the mode current loop is implemented on an analog board and then could be considered as a very “fast” system with respect to the voltage loop.

The switching frequency is 20 kHz, with a minimum “on” time (2.5 μs). The output filter consist in an inductor ($L = 2.23\,\mathrm{mH}$), a capacitor ($C = 165\,\mu\mathrm{F}$) and a resistor ($R_1 = 10\,\Omega$). The load is a variable resistor with $R_2 = 200\,\Omega$ that could be connected or disconnected. The power supply is 200 V with an

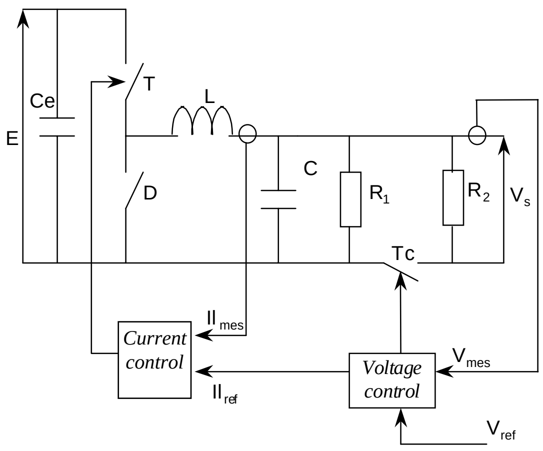

Fig. 1. The dc to dc converter.

input filter ($C_e = 1\mu F$). The maximum inductor current is 10 A, and the voltage controller delivers the current reference Il_{ref}. The control algorithm for output voltage regulation is realised by a DSP TMS320C31 which is implemented for this experimentations and tests on a DS1102 board from Dspace^{TM}. The sampling frequency is 6.6 kHz. The output voltage measurement is filtered by a digital first order filter at 500 Hz frequency.

3. The control principle

3.1. The Buck dc/dc model

Depending on the load, the non reversible Buck dc/dc converter could have different equivalent average models during its operation [5,6]. The following equations describe the difference between continuous current mode, with maximum load (1) and discontinuous current mode with no load (2).

$$\frac{V_s(p)}{Il(p)} = \frac{R}{RCp + 1} \tag{1}$$

$$\frac{V_s(p)}{Il(p)} = \frac{\sqrt{R}A}{RCBp + 1} \tag{2}$$

with

$$B = \frac{1 - \frac{V_s}{E}}{2 - 3 \times \frac{V_s}{E}} \tag{3}$$

$$A = \frac{\sqrt{2L.f.(1 - \frac{V_s}{E})}}{2 - 3 \times \frac{V_s}{E}} \tag{4}$$

3.2. Classical control

In industrial applications, classical controllers are PI, IP or PID. In our case we use IP controller:

$$u(t) = k_p\, e(t) + \frac{k_p}{k_i} \int e(t)\, \mathrm{d}t \tag{5}$$

Here, this controller is tuned for 3 ms of response time, and 0.7 for damping factor.

$$\frac{Il_{\mathrm{ref}}(p)}{\varepsilon(p)} = \frac{K_p(K_i p + 1)}{K_i p} \tag{6}$$

and the reference input is filtered as follows:

$$\frac{V_{\mathrm{Sf}}(p)}{V_{\mathrm{Sref}}(p)} = \frac{1}{K_i p + 1} \tag{7}$$

But the set of parameters obtained for a specific resistor value is not appropriate for another resistor and the desired features are not respected. Then, the control is not very robust, as the resistor value have significant influence on the output behaviour. It can be seen that although the load is a simple but time varying load, the problem is not so simple because system model and parameters are not constant and simultaneously change. Moreover, the model becomes non linear during discontinuous current mode.

To illustrate these control parameters dependence versus the system parameters, Figs. 2 and 3 show the appropriate parameters K_p and K_i for IP control when the gain and time constant of the system model separately change. A special attention should be paid to the particular case of load resistor variation on the buck converter. In this particular type of system, the gain and time constant have non linear coupled variations. The surface for K_p (and K_i) becomes a non-linear curve, marked by the "o" symbols on Figs. 2 and 3.

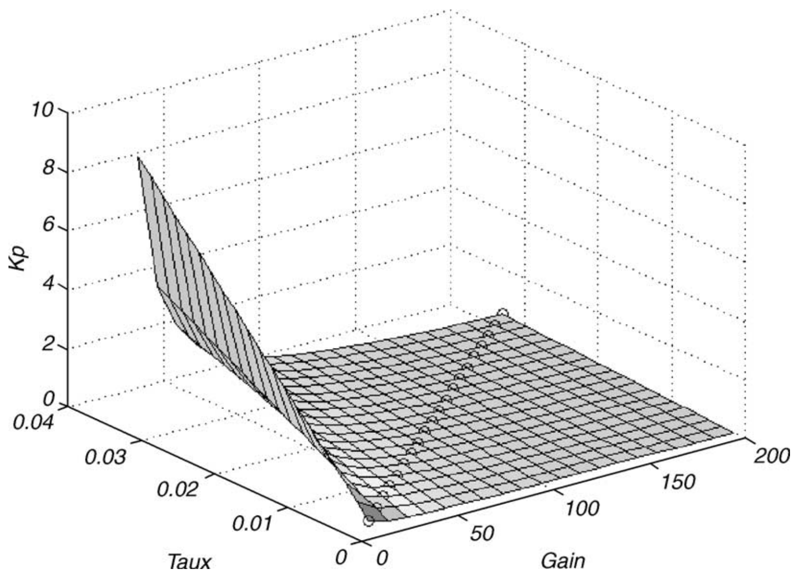

Fig. 2. Control parameters variations vs. gain and time constant.

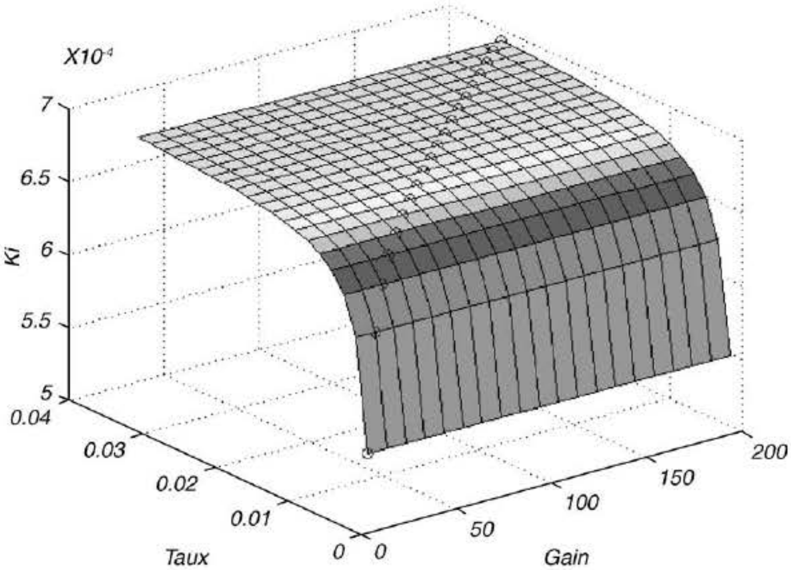

Fig. 3. Control parameters variations vs. gain and time constant.

3.3. Multiple model control

3.3.1. Multiple model control (MMC) principle

The principle MMC is shown Fig. 4. Two controllers C_1 and C_2 have to cooperate to provide the best control action *u* to optimize the performances.

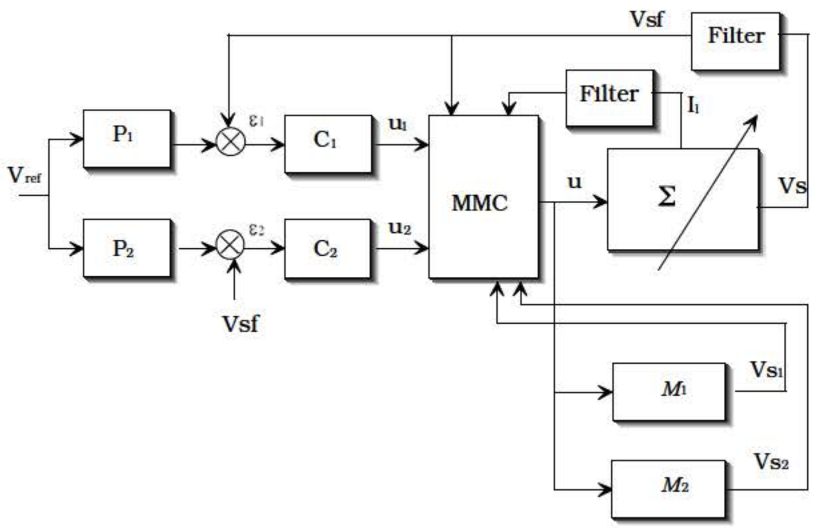

Fig. 4. Block diagram of the Multiple model control.

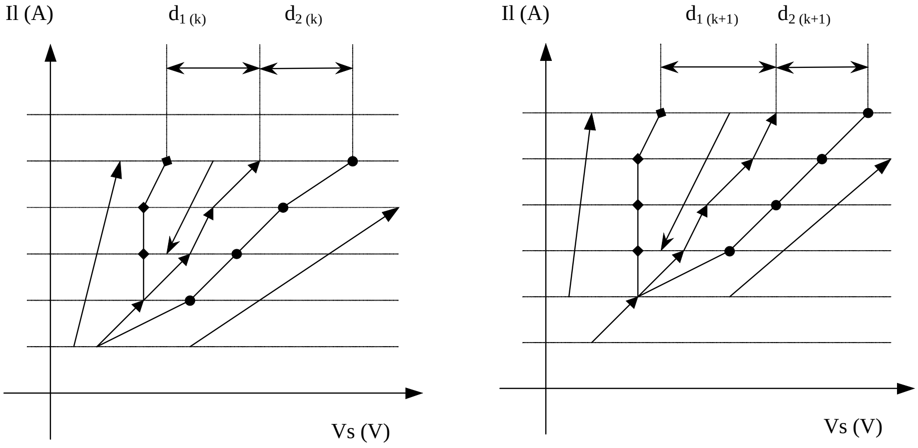

Fig. 5. Model detection principle.

C_1 is tuned for maximum load conditions ($R_2//R_1$) and C_2 is tuned for no load conditions (R_1 disconnected). Two models have signal u as the same control signal than system in order to generate V_{s_1} and V_{s_2}.

3.3.2. *Model detection*

A special procedure is defined to compute the model membership function degree, to check if the system looks like model 1, model 2 or none. At each sampling period, the four previous points (V_s, Il) are kept in memory and compared to the results of model 1 and model 2 simulated behaviours. The result is the distances between the system and the two models, that is to say the membership function activation degree, d_1 and d_2, cf. Fig. 5.

3.3.3. *Fusion control*

The principle of control fusion is very simple. At each sampling instant, C_1 and C_2 controllers give a control action u_1 and respectively u_2 that are mixed to compute the right and optimal value u. The following equations explain the fusion control principle, how to get u from the distances between the actual output voltage of the system V_s and the output of model 1, namely, V_{s_1} and the output of model 2, V_{s_2}.

$$d_i = \sqrt{(V_s)^2 - (V_{s_i})^2} \tag{8}$$

$$Fa_1 = 1 - \frac{d_1}{d_1 + d_2} = \frac{d_2}{d_1 + d_2}; \qquad Fa_2 = 1 - \frac{d_2}{d_1 + d_2} = \frac{d_1}{d_1 + d_2},$$

$$u = \frac{u_1 Fa_1 + u_2 Fa_2}{Fa_1 + Fa_2} = \frac{u_1 d_2 + u_2 d_1}{d_1 + d_2}$$

The theoretical weighting factor (alpha) between the two controllers C_1 and C_2 could be calculated, in order to give an equivalent optimal IP controller. The corresponding relationship between alpha and the resistor value is plotted on Fig. 6. It can be seen that for $R = 10\,\Omega$, alpha is “1” that is to say that the system is completely model 1. For $R = 20\,\Omega$, alpha is 0.5, because the system is half model 1 and half model 2.

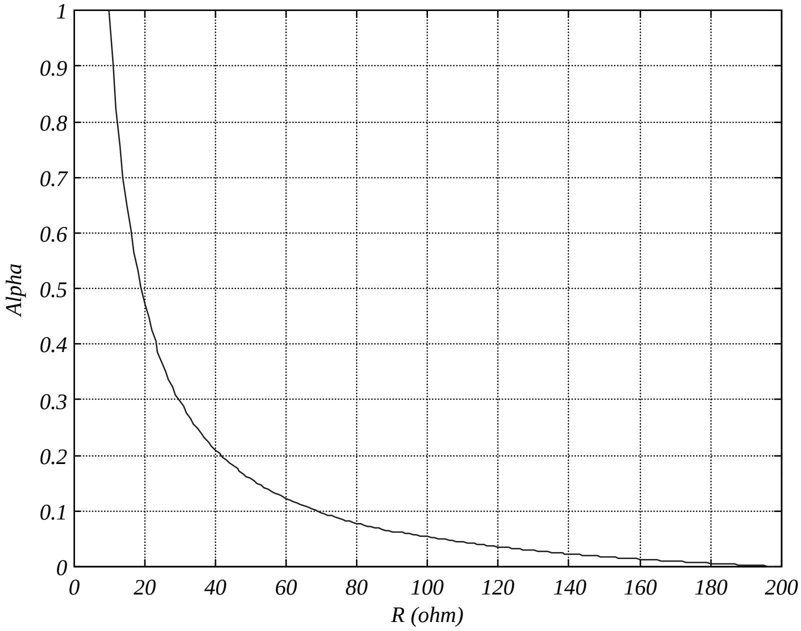

Fig. 6. Theoretical weighting factor between the two controllers C_1 and C_2.

4. Simulation results

Simulation results are obtained from Matlab-Simulink™ softwares, using *S*-functions to generate control signals. A triple test benchmark for the control law is used: nominal load step start, no-load regulation (at $t = t_1 = 35\,\text{ms}$), nominal load regulation (at $t = t_2 = 70\,\text{ms}$); half nominal load, no-load regulation (at $t = t_1 = 35\,\text{ms}$), nominal load regulation (at $t = t_2 = 70\,\text{ms}$); no-load regulation.

Simulation results (Fig. 7) show the voltage output for different controllers and with different loads. One could see that MMC have better performances (lower curves) rather than both of the IP controllers, mainly during step input responses and more slightly during load transients.

It could also be seen that the membership function activation degree, how much the system looks like one model or the other, is correct. For example on the upper figure (Fig. 8), with 10 Ω, model 1 degree is almost 1 and model 2 degree is almost 0. The differences between the theoretical value (1) and the actual value is due to the difference between the average model and the real system operating with an internal current mode control.

5. Experimental results

The experimental behaviour is quite similar to simulations.

Nevertheless on Fig. 9, the MMC on lower curves have better performances rather than that of the IP_1 controller on upper curves (best of IP_1 and IP_2), but mainly during step input responses and more slightly during load transients. Our investigations will then focus in this last part only on step input

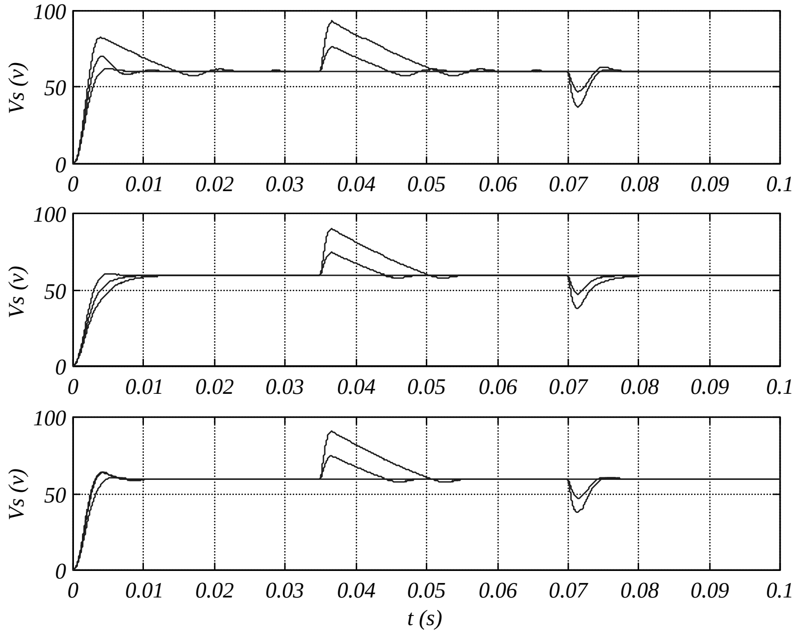

Fig. 7. Output voltage for $V_{s_{ref}} = 30$ and 60 V with IP_1 controller (upper), IP_2 controller (middle), MMC (lower).

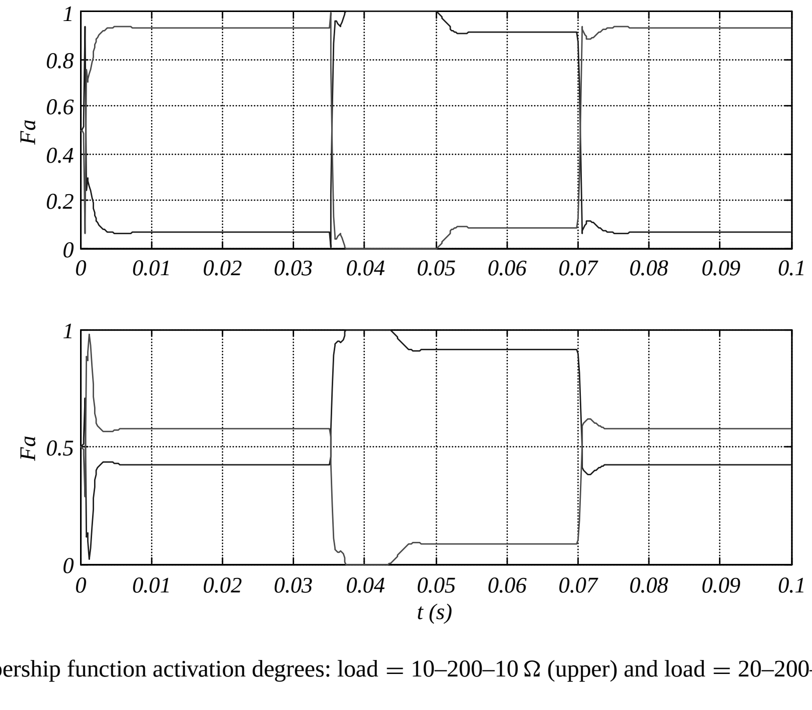

Fig. 8. Membership function activation degrees: load = 10–200–10 Ω (upper) and load = 20–200–20 Ω (lower).

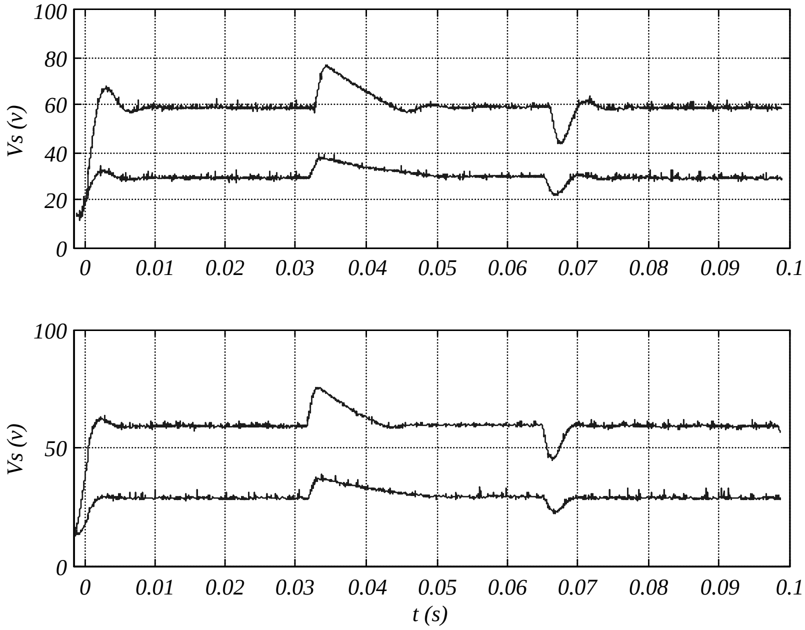

Fig. 9. Output voltage for $V_{s_{ref}} = 30$ and 60 V with IP_1 controller load = 10–200–10 Ω (upper), load = 20–200–20 Ω (middle), load = 200 Ω (lower).

behaviour, trying to show how to keep the same performances, the same behaviour whatever the load could be.

5.1. Step inputs for IP_1 controller (tuned for $R = 10\ \Omega$)

The best response is obviously reached when the system runs with 10 Ω, the load value used to tune the IP_1 controller. Upper curve is good, middle curve is mean and lower curve is bad (overshoot).

5.2. Step inputs for IP_2 controller (tuned for $R = 200\ \Omega$)

This time, the best response is once again reached when the system runs with the specific value it was designed for, that is to say 200 Ω. Upper curve is bad, (too long time response), middle curve is mean and lower curve is good.

5.3. MMC controller: mix of IP_1 and IP_2

Comparing Figs. 10–12 the performances improvement due to the MMC clearly appears. It could be seen on Fig. 12 that the upper curve is good, the middle curve is mean and the lower curve is good once again. In another way, the output waveform and the performances (overshoot, time response, etc.) with the MMC, do not depend any longer on the load.

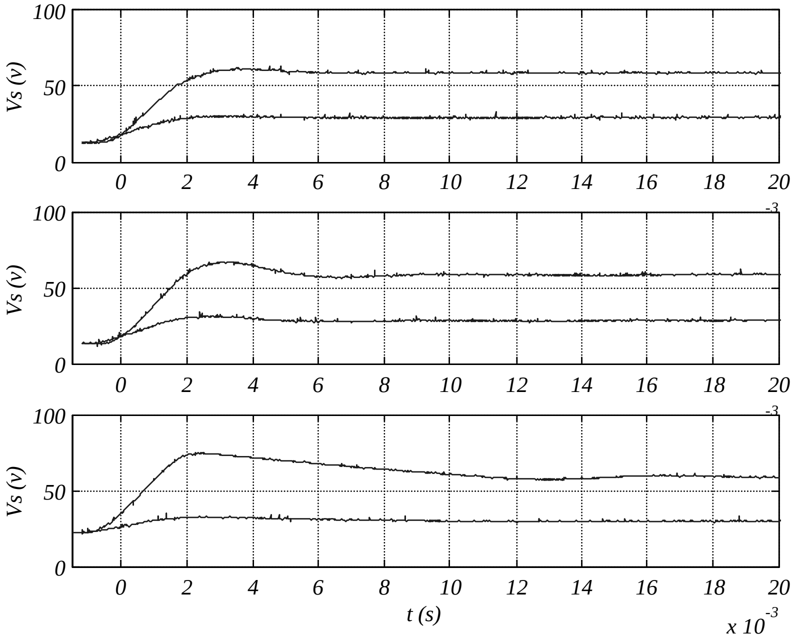

Fig. 10. Output voltage for $V_{s_{ref}} = 30$ and 60 V, IP_1 controller load = 10 Ω (upper), load = 20 Ω (middle) and load = 200 Ω (lower).

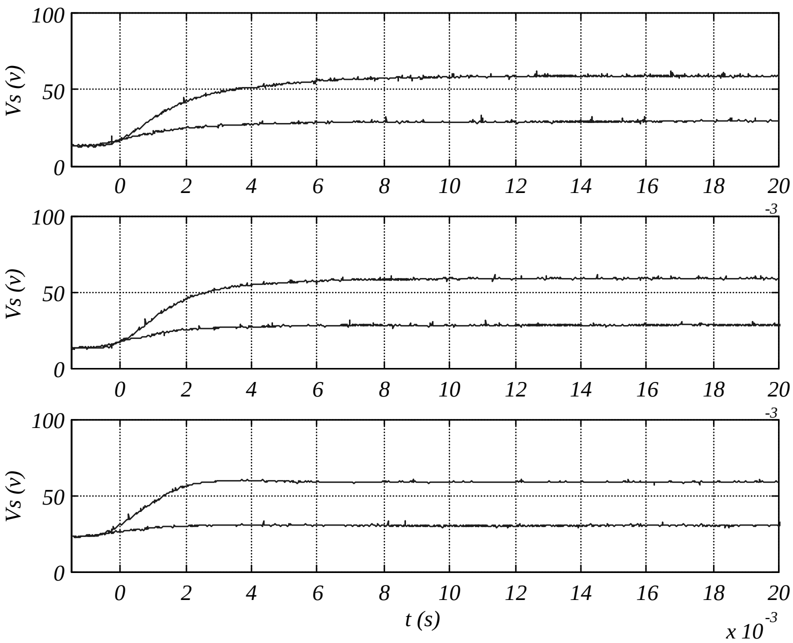

Fig. 11. Output voltage for $V_{s_{ref}} = 30$ and 60 V IP_2 controller load = 10 Ω (upper), load = 20 Ω (middle) and load = 200 Ω (lower).

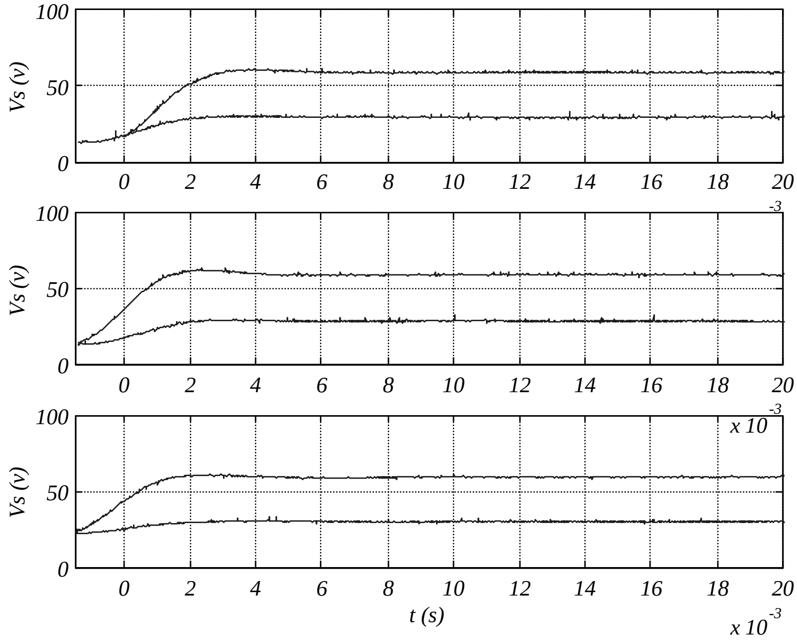

Fig. 12. Output voltage for $V_{s_{ref}} = 30$ and 60 V with MMC load = 10 Ω (upper), load = 20 Ω (middle) and load = 200 Ω (lower).

This phenomenon can also be red in Table 1 where the time response and overshoot values are improved from IP_1 or IP_2 correctors with respect to MMC. The advantage also lies in the fact that these performances remain constant despite the load variations, providing a certain robustness.

As it was seen previously with the experimental results, the designed specific procedure succeed in finding the right membership function activation degree, almost "1" on one hand when $R = 10\,\Omega$ and almost "0" on the other hand when $R = 200\,\Omega$ on the upper Fig. 13. On the lower Fig. 13, the two membership function activation degrees for model 1 and model 2 are 0.5 because the load is 20 Ω, half the maximum load.

Table 1
Performance measurements with step input for different loads during step inputs

60 V set point	Type of controller	Step input with different loads		
		10 Ω	20 Ω	200 Ω
Response time 5% (ms)	IP_1	3.35	5.35	8.7
	IP_2	7.8	6.5	3.1
	MMC	3.5	3.2	3.1
Overshoot (%)	IP_1	2.5	11.33	24.17
	IP_2	0	0	1.67
	MMC	1.67	1.8	1.33

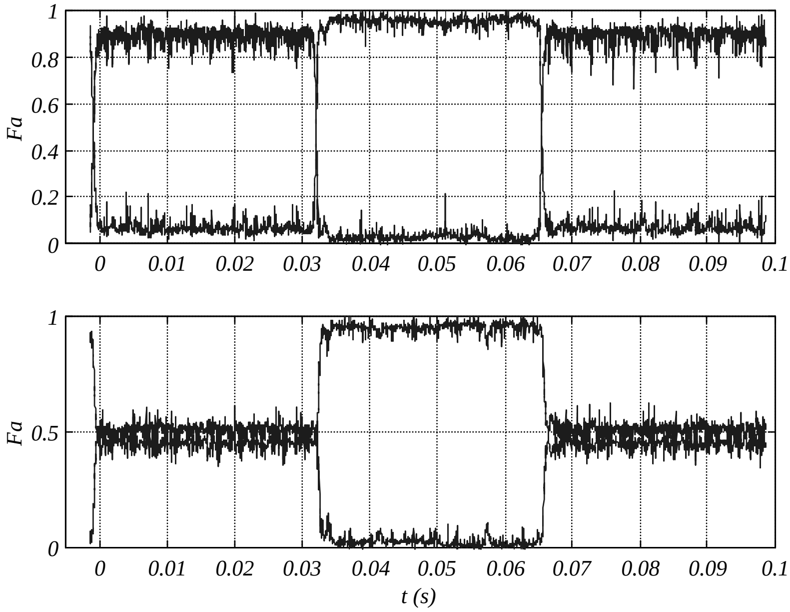

Fig. 13. Membership function activation degrees: load = 10–200–10 Ω (upper) and load = 20–200–20 Ω (lower).

6. Conclusion

The original method proposed in this paper mix two simple controllers, in order to obtain a better control law, is efficient on reference changes during step input. The specific procedure necessary to determine what model the system looks like, has good performances. The whole system will increase its performances using a combined approach, the one presented in this paper and the soft switching given in [3].

References

[1] B. Robyns, F. Berthereau, J.P. Hautier, H. Buyse, A fuzzy logic-based multimodel field orientation in an indirect F.O.C. of an induction motor, IEEE Trans. Ind. Electron. 47 (2) (2000) 380–388.
[2] D. Hissel, P. Maussion, J. Faucher, in: Proceedings of the Presentation at ISIE'99 on Speed Ripples Reduction of a Non-linear Loaded Synchronous Motor Trough Fuzzy Algorithm Commutation, July 99, Bled, Slovenie.
[3] D. Alejo, P. Maussion, J. Faucher, in: Proceedings of the Presentation at EPE'01 on Control Laws Soft Switching for a dc/dc Converter, August 2001, Graz, Austria.
[4] M. Ksouri-Lahmari, A. El Kamel, M. Benrejeb, P. Borne, in: Proceedings of the Presentation at IEEE-SMC'97 on Multimodel, Multicontrol Decision Making in System Automation, Orlando, FL, USA, October 1997.
[5] J.P. Ferrieux and F. Forest, "Alimentation à découpage, Convertisseurs à résonance. Edition Dunod.
[6] H Bühler, Réglage électronique de command", Presses Polytechniques Romandes.